Date: June 27, 2009

Constraining the MSSM with universal gaugino masses and implication for searches at the LHC

G. Bélanger[1], F. Boudjema[1], A. Pukhov[2], R. K. Singh[1,3]

1) LAPTH, Univ. de Savoie, CNRS, B.P.110, F-74941 Annecy-le-Vieux, France
2) Skobeltsyn Inst. of Nuclear Physics, Moscow State Univ., Moscow 119992, Russia
3) Institut für Theoretische Physik und Astrophysik, Universität Würzburg, D-97074 Würzburg, GERMANY

Abstract

Using a Markov chain Monte Carlo approach, we find the allowed parameter space of a MSSM model with seven free parameters. In this model universality conditions at the GUT scale are imposed on the gaugino sector. We require in particular that the relic density of dark matter saturates the value extracted from cosmological measurements assuming a standard cosmological scenario. We characterize the parameter space of the model that satisfies experimental constraints and illustrate the complementarity of the LHC searches, B-physics observables and direct dark matter searches for further probing the parameter space of the model. We also explore the different decay chains expected for the coloured particles that would be produced at LHC.

1 Introduction

Among the large number of theoretical models proposed to either solve the hierarchy problem and/or explain dark matter with a new stable particle, the minimal supersymmetric model (MSSM) remains one of the favourite. Supersymmetry not only provides a solution to both these problems but also predicts new physics around the TeV scale. The main drawback of the MSSM apart from the lack of evidence for supersymmetric particles is the large number of unknown parameters most of which describe the symmetry breaking sector. With the improved sensitivities of dark matter searches in astroparticle experiments [1, 2, 3, 4, 5, 6], the precise determination of the DM relic density from cosmology [7, 8, 9], the latest results from the Tevatron [10, 11] and the precision measurements, large regions of the parameter space of the supersymmetric models are being probed. This will continue in the near future with a number of direct and indirect detection experiments improving their sensitivities [12, 13, 14, 15] and most importantly with the LHC starting to take data. The LHC running at the full design energy of 14TeV offers good prospects for producing coloured supersymmetric particles lighter than 2-3 TeV, for discovering one or more Higgs scalars [16, 17] and for measuring the rare processes in the flavour sector, in particular in B-physics [18]. Furthermore some properties of the sparticles, in particular mass differences can be measured precisely in some scenarios [16, 17].

The first studies that extracted constraints on supersymmetric models worked in general within the context of the MSSM embedded in a GUT scale model such as the CMSSM [19, 20, 21]. After specifying the fundamental model parameters at the high scale, the renormalisation group equations are used to obtain the weak scale particle spectrum. This approach provides a convenient framework for phenomenological analyses

as the number of free parameters is reduced drastically compared to the general MSSM (from O(100) to 4 and 1/2 parameters in the case of the CMSSM). The drawback is that one is often confined to very specific scenarios, for example in the CMSSM the LSP is dominantly bino over most of the parameter space. This has important consequences for the dark matter relic abundance. Furthermore it was customary to choose some specific values for some of the MSSM or even the SM parameters for a convenient representation of the parameter space in two-dimensions. While the link between specific observables and allowed region of parameter space is easier to grasp in this framework, the allowed parameter space appeared much more restrictive than if all free parameters were allowed to vary.

In the last few years efficient methods for exploring multi-dimensional parameter space have been used in particle physics and more specifically for determining the allowed parameter space of the CMSSM. This approach showed that the often narrow strips in parameter space obtained when varying only two parameters at a time fattened to large areas [22, 23, 24, 25] after letting all parameters of the CMSSM and the SM vary in the full range. With this efficient parameter space sampling method it becomes possible to relax some theoretical assumptions and consider the full parameter space of the MSSM. Because the number of experimental constraints on TeV scale physics is still rather limited it seems a bit premature to go to the full fledge $\mathcal{O}(100)$ parameters of the MSSM or even to the 19 parameters that characterize the model when assuming no flavour structure and equality of all soft parameters for the first and second generations of sfermions (for an approach along these lines see [26, 27]). Furthermore many parameters, for example those of the first and second generations of squarks, once chosen to be equal to avoid strong flavour-changing neutral current constraints, do not play an important role in the observables selected to fit the model. Here we consider a model where input parameters of the MSSM are defined at the weak scale and we add some simplifying assumptions: common slepton masses ($M_{\tilde{l}_R} = M_{\tilde{l}_L} = M_{\tilde{l}}$) and common squark masses ($M_{\tilde{q}_R} = M_{\tilde{q}_L} = M_{\tilde{q}}$ at the weak scale for all three generations and universality of gaugino parameters at the GUT scale. This implies the following relation between the gaugino masses at the weak scale, $M_2 = 2M_1 = M_3/3$. We furthermore assume that A_t is the only non-zero trilinear coupling. While, as we just argued, the first assumption should not impact much our analysis, the second should certainly be considered as a theoretical bias. This assumption is however well motivated in the context of models defined at the GUT scale. Most importantly in our approach we keep the higgsino parameter μ and the gaugino mass M_2 as completely independent parameter. The relation between the gaugino and higgsino parameters is what determines the nature of the LSP and plays an important role in determining the LSP-LSP annihilation in the early universe. In that sense our model has many similarities with the non-universal Higgs model which also has μ and M_2 as independent parameters [28].

The observables selected to constrain the model include the relic density of dark matter, Ωh^2, direct searches for Higgs and new particles at colliders, searches for rare processes such as the muon anomalous magnetic moment as well as various B-physics observables. Note that the dark matter relic abundance is computed within the standard cosmological scenario. The direct detection of dark matter while providing stringent constraint on the model introduces additional unknown parameters both from astrophysics and from strong interactions. We therefore prefer to consider the direct detection rate as an observable to be predicted rather than as a constraint keeping in mind that folding in the astro-

physical and hadronic uncertainty could however easily introduce an order of magnitude uncertainty in that prediction [29, 30].

We find that each individual parameter of the MSSM model is only weakly constrained, in particular the parameters of the sfermion sector. The very large allowed parameter space only reflects the still poor sampling of the total parameter space by experiments. The neutralino sector is better constrained with a preferred value for the LSP of a few hundred GeV's and a small likelihood for masses above 900GeV, similarly charginos above 1.2TeV are disfavoured. We also find a lower limit on the pseudo-scalar mass as well as on $\tan\beta$. Furthermore some correlations between parameters of the model are observed, most notably the one between μ and the gaugino mass. This is because those two parameters determine the higgsino content of the LSP.

After having determined the allowed parameter space, we examined the predictions for direct detection as well as for LHC searches both in the Higgs and SUSY sector as well as for B-physics observables. Although each type of search can only probe a fraction of the total parameter space we find a good complementarity between the different searches with less than 10% of scenarios leading to no signal. For example large signals for direct detection are expected in the mixed bino/Higgsino LSP scenario that are hard to probe at the LHC. The LHC searches in the SUSY and Higgs sector are also complementary and B-observables are specially useful in scenarios with large $\tan\beta$ and a pseudoscalar that is not too heavy. The predictions for SUSY searches can be different from that expected in the constrained CMSSM with in particular a large fraction of models that only have a gluino accessible at LHC, the squarks being too heavy. To ascertain how experiments that will take place in the near future could further constrain the parameter space of the model we consider specific case studies. For example we consider the impact of a signal in $B(B_s \to \mu^+\mu^-)$ at Tevatron or of the observation of a signal in direct detection experiments. Finally we examine in more details the SUSY signals at the LHC, analysing the preferred decay chains for models that have either a gluino or a squark within the reach of the LHC. In this analysis we did not include the constraints from indirect detection experiments because the rates predicted feature a strong dependence on additional quantities such as the dark matter profile or the boost factor. The predictions for the rates for $\bar{p}, e^+, \gamma$ will be presented in a separate publication [31].

The paper is organised as follows. The model and the impact of various constraints are described in section 2. The method used for the fit is described in section 3. The results of the global fits are presented in section 4 together with the impact of a selected number of future measurements. The SUSY signatures are detailed in section 5. The conclusion contains a summary of our results.

2 Model and constraints

We consider the MSSM with input parameters defined at the weak scale. We assume minimal flavour violation, equality of the soft masses between sfermion generations and unification of the gaugino mass at the GUT scale. The latter leads to $M_2 = 2M_1 = M_3/3$ at the weak scale (relaxing this assumption is kept for a further study). We allow for only one non-zero trilinear coupling A_t. For the b-squark the mixing which is $\propto A_b - \mu\tan\beta$ is driven in general by $\mu\tan\beta$ rather than by the trilinear coupling, this approximation is however not very good in the small sample of models with $\mu \approx 100$ GeV. Note also

that the Higgs mass at high $\tan\beta$ can show some dependence on the sbottom mixing. For first and second generations of squarks the mixing which depends on fermions masses is negligible except for the neutralino-nucleon cross section since the dominant contributions to the scalar cross section are also dependent on fermion masses. However since the squark exchange diagram is usually subdominant as compared to Higgs exchange, the neglected contribution of the trilinear coupling falls within the theoretical uncertainties introduced by the hadronic matrix elements [30]. Similarly neglecting the the muon trilinear mixing, A_μ, could affect the prediction for δa_μ but this effect is not large compared with the uncertainties on the value extracted from measurements. The top quark mass m_t is also used as an input although it has a much weaker influence on the results than in the case of GUT scale models. For the latter the top quark mass enters the renormalization group evolution and can have a large impact on the supersymmetric spectrum in some regions of the parameter space. In the general MSSM the top quark mass mainly influences the light Higgs mass. We fix $\alpha_s(M_Z) = 0.1172$ and $m_b = 4.23$ GeV. The free parameters of our MSSM model with unified gaugino masses, MSSM-UG, are

$$\mu, M_2, M_{\tilde{l}}, M_{\tilde{q}}, A_t, \tan\beta, M_A, m_t \tag{1}$$

The range examined for each of these parameters is listed in Table 1. MSSM-UG has a far more restricted set of paramters than the general MSSM, still this model will show how the possibilities for SUSY scenarios open up. The observables that will be used in the fit are listed in Table 2. We first review the expectations for the role of each observable in constraining the MSSM parameter space.

Table 1: Range of the free MSSM-UG parameters.

Symbol	stands for	General range
μ	μ parameter	$[-3000, 3000]$ GeV
M_2	Gaugino mass, $2M_1 = M_2 = M_3/3$	$[30, 2000]$ GeV
$M_{\tilde{l}}$	Common slepton mass, $M_{\tilde{l}} = m_{\tilde{\ell}_{L,R}}$	$[50, 4000]$ GeV
$M_{\tilde{q}}$	Common squark mass, $M_{\tilde{q}} = m_{\tilde{q}_{L,R}}$	$[50, 4000]$ GeV
A_t	Trilinear coupling of $\tilde{t}$	$[-3000, 3000]$ GeV
$\tan\beta$	$\tan\beta$	$[5, 65]$
M_A	Mass of CP-odd Higgs boson	$[100, 2000]$ GeV
m_t	mass of t-quark	$[165, 180]$ GeV

The most powerful constraint is Ωh^2. Since in the MSSM with gaugino universality there are four different mechanisms for efficient neutralino annihilation each calling for a different combination of SUSY parameters, each individual parameter is weakly constrained when exploring the full parameter space of the model. The main mechanisms for neutralino annihilation are:

- annihilation of a bino LSP into fermion pairs, this necessitates light right-handed sfermions.

- annihilation of a mixed bino/higgsino into W pairs, this means $\mu \approx M_1$. Some contribution from chargino and neutralino coannihilations is also expected.

- annihilation near a (light or heavy) Higgs resonance, a LSP with a non-zero higgsino component is required but the higgsino fraction can be very small if $m_{\tilde{\chi}_1^0} \approx m_h/2$. For heavy Higgs exchange this process is more efficient at large $\tan\beta$ due to the enhanced couplings of the heavy Higgs to b-quarks and τ leptons.

- Coannihilation with sfermions, this usually means those of the third generation since they are lighter due to mixing. Recall that we are assuming only one slepton mass $M_{\tilde{l}}$ and one squark mass $M_{\tilde{q}}$.

The lower limit on the Higgs mass from LEP strongly constrains the small $\tan\beta$ region. The upper range for the top quark mass and/or a large mixing in the stop sector are favoured. The latter means large values of $|A_t|$.

The muon anomalous magnetic moment still indicates a 3σ deviation from the SM expectations [32]. The SUSY loop contributions can lead to $\delta a_\mu > 0$ when sparticles are light. This is the case for the chargino/sneutrino loop and the neutralino/smuon loop when $\mu > 0$. The latter is enhanced at large values of $\tan\beta$, in this case it is easier to accomodate $\delta a_\mu > 0$ even with a SUSY spectrum at TeV scale. Recall that we have neglected A_μ, although the mixing is usually dominated by $\mu\tan\beta$, this introduces some restriction on the parameter space.

The branching ratio for $B(b \to s\gamma)$ depends on the squark and gaugino/Higgsino sector as well as on the charged Higgs. A light pseudoscalar mass is permitted only if squarks are light as well. The squarks then partially cancel the large pseudoscalar contribution but only for $\mu > 0$. Furthermore when $\mu > 0$, the chargino contribution is negative relative to the SM one so $B(b \to s\gamma)$ can drop too low for light charginos. This is particularly true when A_t is large and negative, meaning a large mixing in the stop sector.

The process $B(B_s \to \mu^+\mu^-)$ receives SUSY loops contributions from Higgs exchange as well as from chargino and sfermions. In particular the amplitude for Higgs exchange is enhanced as $\tan^3\beta$. The largest contribution are therefore expected for large $\tan\beta$ and light M_A, particularly for light charginos and sleptons.

In the MSSM, the branching ratio for $B_u \to \tau\nu_\tau$ is suppressed relative to the standard model prediction by the charged Higgs contribution. This contribution is enhanced as $\tan^2\beta$. We will use the observable $R(B_u \to \tau\nu_\tau)$ which gives the ratio between the SUSY and SM predictions. Due to large uncertainties in hadronic matrix elements the standard model branching fraction is not known with a good precision, so this observable is not as powerful as other B-physics observables to constrain the parameter space of the MSSM.

LEP limits on the light Higgs and on sparticles constrain the chargino and neutralino sector as well as the charged sfermions. We have not included the recent Tevatron limits on the squark and gluino mass as well as the limits on the chargino mass from the trilepton search. When presenting our results we will comment on the impact of the new Tevatron results. [1]

[1]Note that the trilepton search in $pp \to \tilde{\chi}_1^+\tilde{\chi}_2^0$ extends the LEP constraint on the chargino mass only when sfermions are light, no constraint is found in the large scalar mass limit (large m_0) at least in the context of the CMSSM. The large fraction of our models which have heavy squarks will therefore not be probed by the Tevatron even if they feature light neutralinos and charginos.

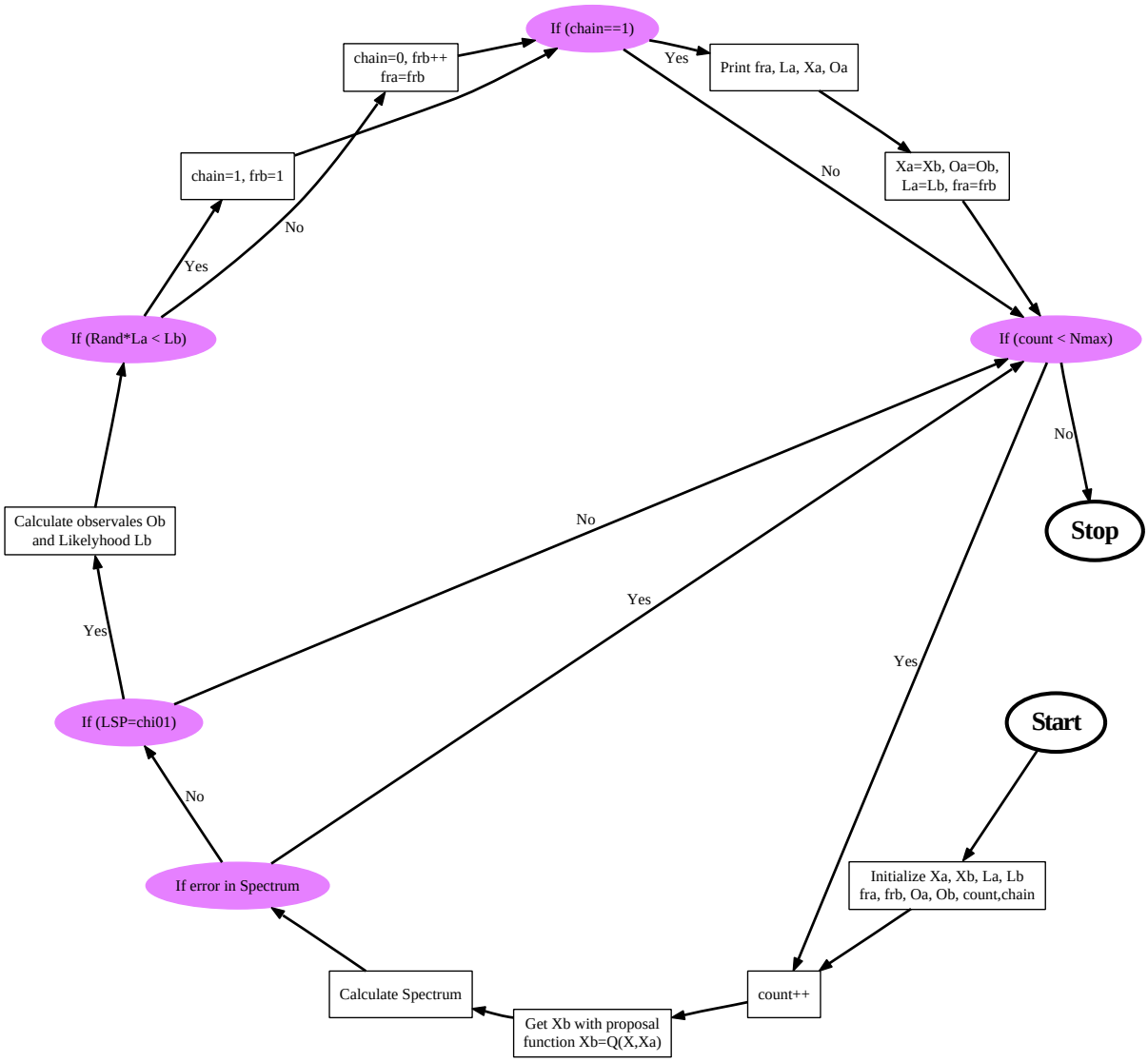

Figure 1: Details of the MCMC algorithm used in this paper. `Xa` and `Xb` are the points in the parameter space, `Oa` and `Ob` are the values of the observables at points `Xa` and `Xb` respectively, `La` and `Lb` are corresponding likelihoods and `fra` and `frb` are the frequencies at two points.

3 Parameter sampling method

In this section we attempt to motivate the MCMC method in a heuristic way, for a detailed treatment see Ref. [33]

The likelihood L is the probability distribution function (PDF) $p(d|m)$ for a data set d being reproduced by an assumed model m. In our case, we assume the model m =MSSM-UG and the data set to be reproduced is given in Table 2. This is a *top-down* approach where by varying the model parameters we find a suitable m to maximise $p(d|m)$. However, in a *bottom-up* approach one would like to know the probability of model m being correct once given the data d, *i.e.* $p(m|d)$. From Bayes' theorem we have

$$p(m|d) = p(d|m)\frac{p(m)}{p(d)},$$

where $p(m)$ is the (absolute) probability of the model m being correct and $p(d)$ is the total probability of reproducing the data d for all possible models. The $p(d)$ is *hard* to estimate since it requires knowledge of all possible models. Thus, the absolute value of $p(m|d)$ is hard to estimate. However, it is possible to estimate the *relative correctedness* of a model m_1 against another model m_2 given the data d by taking the ratio

$$\frac{p(m_1|d)}{p(m_2|d)} = \frac{p(d|m_1)\ p(m_1)}{p(d|m_2)\ p(m_2)}.$$

For simplicity, we take $p(m_1) = p(m_2)$, that is the probability of two models being correct is same or we chose a flat prior over the model space. In this paper this translates to using a flat prior over the parameter space of MSSM-UG as listed in Table 1. Thus with flat prior we have

$$\frac{p(m_1|d)}{p(m_2|d)} = \frac{L(m_1)}{L(m_2)}.$$

This clearly hints that if we sample the parameter space using a directed random walk with transition probability proportional to $\min(1, L(m_1)/L(m_2))$, the sampling density will be proportional to the likelihood ratio or the relative correctedness of the model. The details can be found in [33] and a representation of the algorithm used is given in Fig. 1.

There are two points in order: For the sampling density to be proportional to the ratio of the likelihoods the proposal PDF, $Q(\mathbf{X}, \mathbf{X_a})$, should be symmetric about $\mathbf{X_a}$, where $\mathbf{X}, \mathbf{X_a}$ are point in the parameter space. We use the Gaussian distribution in each parameter direction and the proposal PDF looks like:

$$Q(\mathbf{X}, \mathbf{X_a}) = \prod_i \exp\left[\frac{-(X^i - X_a^i)^2}{2\ (\Delta X^i)^2}\right].$$

The second point is about the definition of likelihood. The likelihood L is a product of likelihood for each of the observables. For the observable with definite measurement the likelhood function is a Gaussian

$$\mathbf{G}(O, O_{exp}, \Delta O) = \exp\left[\frac{-(O - O_{exp})^2}{2\ (\Delta O)^2}\right].$$

Here, O_{exp} is the central value of the observable, ΔO is the 1σ error and O is the value of the observable at the proposed point $\mathbf{X}$ in the parameter space. For observables with upper/lower limits the likelihood function is a smooth step-like fuction

$$\mathbf{F}(O, O_{exp}, \Delta O) = \frac{1}{1 + \exp[\pm(O - O_{exp})/\Delta O]}$$

The +ve sign is for the lower limit and the $-$ve is for the upper limit. Here O_{exp} is the 95% exclusion limit and ΔO is about 1% of O_{exp} to roughly emulate the 95% exclusion limit. The list of observables used to calculate the likelihood is given in Table 2 alongwith the correponding experimental values or limits.

4 Results

We have first scanned linearly over the 8 parameters of the MSSM-UG using the Markov Chain Monte Carlo (MCMC) method just described. The particle spectrum was computed

by SoftSusy2.0 [34] and fed to micrOMEGAs2.2 [35, 36, 30] for the computation of all DM observables as well as of constraints on the parameters of the supersymmetric model. The SM value for the branching $B(b \to s\gamma)$ calculated in [35] was shifted in order to match the NNLO result of [37].

The range chosen for all parameters is listed in Table 1 and the six observables used in the fit listed in Table 2. In addition we have imposed the LEP limits on sparticles ($m_{\tilde{\chi}_1^+}$, $m_{\tilde{l}}$...) as defined in micrOMEGAs and for the likelihood we have assumed a binary step function. We then examined the allowed regions for each input parameter as well as the predictions for physical parameters and observables. We have not imposed the Tevatron limit on gluino and squarks $m_{\tilde{g}} > 308$ GeV and $m_{\tilde{q}} > 379$ GeV [38]. However after fitting the model we have checked a posteriori that these constraints did not affect much our analysis. Because of the universality condition the gluino mass limit is always satisfied while the squark limit is not satisfied in less than one per-mil of our scenarios.

Table 2: Observables used in the fit.

Observable	Limit	Likelihood function
δa_μ	$(27.8 \pm 8.5) \times 10^{-10}$	$\mathbf{G}(x, 27.8 \times 10^{-10}, 8.5 \times 10^{-10})$
$B(b \to s\gamma)$	$(3.55 \pm 0.24) \times 10^{-4}$	$\mathbf{G}(x, 3.55 \times 10^{-4}, 0.24 \times 10^{-4})$
Ωh^2	0.113 ± 0.0105	$\mathbf{G}(x, 0.113, 0.0105)$
$B(B_s \to \mu^+\mu^-)$	$\leq 0.8 \times 10^{-7}$	$\mathbf{F}(x, 0.8 \times 10^{-7}, -0.8 \times 10^{-9})$
$R(B \to \tau^+\nu)$	1.11 ± 0.52	$\mathbf{G}(x, 1.11, 0.52)$
m_h	≥ 114.5 GeV	$\mathbf{F}(x, 114.5, 0.6)$
m_t	171.4 ± 2.1 GeV	$\mathbf{G}(x, 171.4, 2.1)$

Table 3: Range of the MSSM parameters.

Parameter	68% C.L.		95% C.L.	
μ	197.7	1193	-983.5	2471
M_2	259.8	1077	119.6	1845
$M_{\tilde{l}}$	398.4	2270	225.4	3700
$M_{\tilde{q}}$	1824	3602	1236	3938
A_t	-1735	2239	-2785	2876
$\tan\beta$	19.5	65.0	8.15	65.0
M_A	537.1	1489	370.2	1904
m_t	169.6	173.7	167.6	175.6

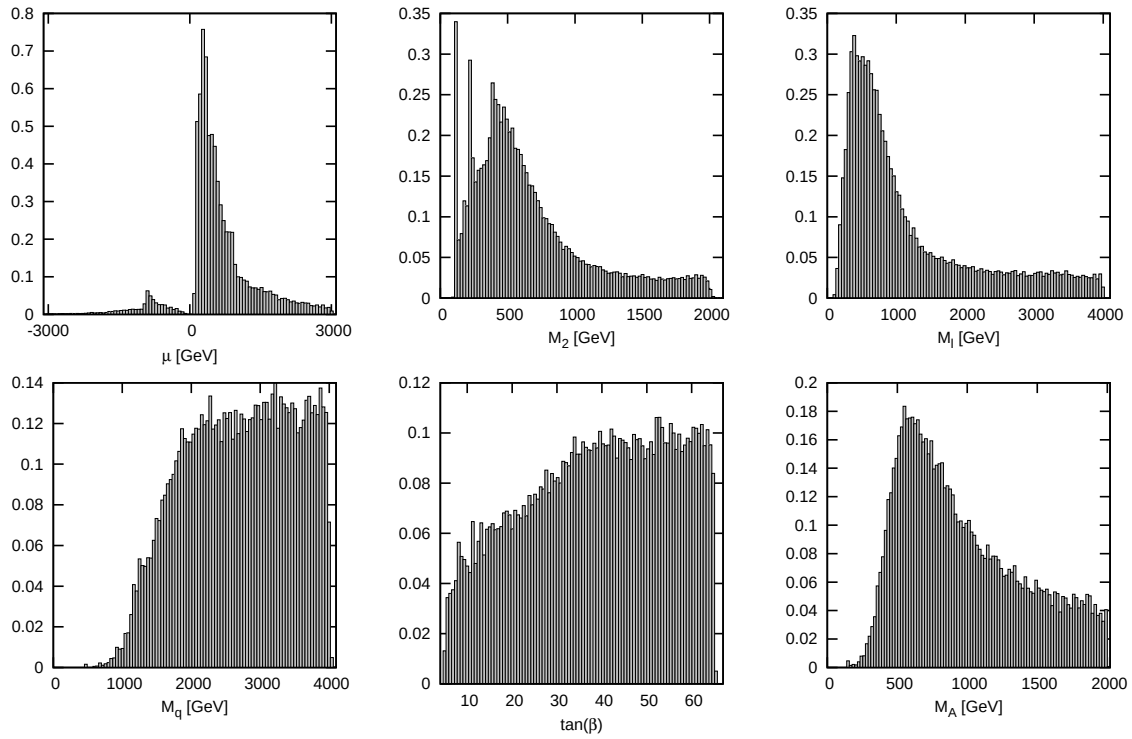

Figure 2: Likelihood function for the model parameters, from top left: μ,M_2,$M_{\tilde{l}}$,$M_{\tilde{q}}$, $\tan\beta$,M_A, all dimensionfull parameters in GeV.

4.1 The allowed parameter space of the MSSM

We found wide allowed regions for each model parameter, the distributions are displayed in fig. 2 and the 68% and 95% limits in Table 3.

- As expected, $\mu > 0$ is preferred, this is mainly due to the $B(b \to s\gamma)$ and δa_μ constraints. Note however that one can get a reliable global fit even with $\delta a_\mu = 0$ so that the 95%C.L. extends to the negative μ region, see Table 1.

- The gaugino mass reaches almost the maximum value probed, $M_2 < 1845$ GeV at 95%C.L. Charginos above the TeV scale are somewhat disfavoured (see the 68% C. L. at 1.1 TeV) because they give little contribution to δa_μ, furthermore the light neutralinos LSP annihilate more efficiently except when they have a large Higgsino component or can annihilate near a resonance.

- The slepton mass distribution is peaked at 500GeV with a long tail that extends to almost the upper limit of the region scanned. The sleptons just above the LEP limit are disfavoured with 225GeV $< M_{\tilde{l}} <$ 3700 GeV at 95%C.L. This shows that although light sleptons can contribute to the annihilation of a bino LSP and to δa_μ, present data can be accomodated with heavy sleptons.

- Heavy squarks are preferred with $M_{\tilde{q}} > 1.24$ TeV at 97.5%C.L. Quarks below the TeV scale tend to give too large corrections to B-physics observables and in particular to $B(b \to s\gamma)$. Although the quark contribution can be compensated by that of a light pseudoscalar, this requires fine-tuning and has a small likelihood. There

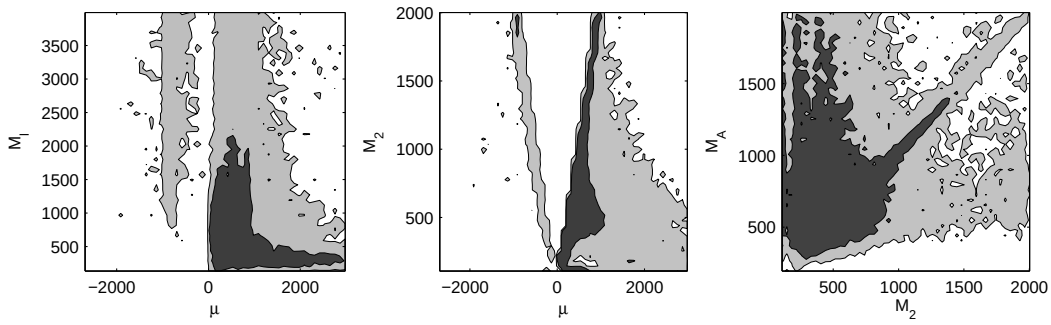

Figure 3: 2d-likelihood functions for a) $M_{\tilde{l}} - \mu$ b)$M_2 - \mu$ c)$M_A - M_2$ showing the 68%C.L.(dark grey) and 95% C.L. (light grey). All parameters in GeV.

is no upper limit on the squark mass as it can reach the upper limit of the range used in the scan, 4 TeV.

- Light pseudoscalars are disfavoured with $M_A \geq 370$ GeV at 97.5% C.L. While it is possible to have a good fit to the data with lighter pseudoscalar masses this occur only after fine tuning the sfermion masses in order to satisfy both δa_μ and $B(b \to s\gamma)$. Therefore these models have a small likelihood.

- The distribution for $\tan\beta$ is skewed towards the upper range and $\tan\beta > 8.15$ at 97.5% C.L. Large values of $\tan\beta$ make it easier to escape the LEP bound on the Higgs mass, facilitate annihilation of the LSP through Higgs exchange and can also help explain δa_μ.

- There are no preferred value for A_t although the distribution is skewed towards $A_t > 0$, see Table 3.

A few correlations among input parameters are observed. These are driven to a large extent by the relic density constraint. First μ and $M_{\tilde{l}}$ are correlated: a large μ requires light sleptons while heavy sleptons need μ not much above the TeV scale. When sleptons are heavy the LSP must have a higgsino component to annihilate efficiently. Conversely when μ is large and the LSP is bino, light sleptons are needed for efficient annihilation into fermion pairs. Second M_2 is also correlated with μ and M_A: when M_2 exceeds 1.2TeV, one needs either $|\mu| \approx M_2/2 \approx M_1$ or $M_2 \simeq M_A$. The first correlation is strong and means that a heavy LSP with a significant higgsino component annihilates efficiently. The second correlation corresponds to $m_{\tilde{\chi}_1^0} \approx M_A/2$ with the LSP annihilating near a heavy Higgs resonance. This correlation is weak as we have just mentionned, other large values of M_2 are allowed when the LSP has a large higgsino component.

4.2 The particle spectrum

From this allowed parameter space we can determine the favoured region for the masses of new particles that can be searched for at LHC.

- The light Higgs is SM like and $m_h = 120.2^{+4.6}_{-4.9}$ GeV at 95%C.L.

Table 4: The 68% and 95% allowed range for sparticle masses and for the higgsino fraction.

Mass	68% C.L.		95% C.L.	
m_h	117.6	122.6	115.3	124.8
m_H	537	1489	370	1900
$m_{\tilde{\chi}_1^0}$	52.2	522	52.2	874
$m_{\tilde{\chi}_2^0}$	104	756	104	1180
$m_{\tilde{\chi}_3^0}$	269	1300	158	2500
$m_{\tilde{\chi}_4^0}$	412	1650	265	2510
$m_{\tilde{\chi}_1^+}$	103	749	103	1180
$m_{\tilde{\chi}_2^+}$	410	1640	262	2490
$m_{\tilde{e}_L}$	410	2280	235	3710
$m_{\tilde{e}_R}$	406	2270	236	3700
$m_{\tilde{\tau}_1}$	103	2260	103	3690
$m_{\tilde{\tau}_2}$	457	2280	276	3710
$m_{\tilde{u}_L}$	1840	3650	1230	3990
$m_{\tilde{u}_R}$	1850	3660	1240	4000
$m_{\tilde{d}_L}$	1850	3670	1240	4010
$m_{\tilde{d}_R}$	1850	3660	1240	4000
$m_{\tilde{b}_1}$	1820	3620	1200	3960
$m_{\tilde{b}_2}$	1850	3650	1250	3990
$m_{\tilde{t}_1}$	1770	3590	1130	3930
$m_{\tilde{t}_2}$	1880	3660	1300	4000
$m_{\tilde{g}}$	952	3320	478	5400
f_H	$1.58\ 10^{-3}$	0.297	$3.39\ 10^{-4}$	0.659

- The LSP mass is in the range 52 GeV $< m_{\tilde{\chi}_1^0} <$ 873 GeV at 95%C.L. The lower bound results from the assumption of GUT scale gaugino mass universality and the LEP limit on charginos. The peak in the distribution around 55 GeV corresponds to LSP annihilation near a light Higgs resonance.

- The lightest chargino (as well as $\tilde{\chi}_2^0$) could be just above the LEP reach and lies below $m_{\tilde{\chi}_1^+} < 1182$ GeV at 97.5%C.L. There is a peak in the distribution near 100GeV which is correlated with the LSP peak correponding to annihilation near the light Higgs.

- The gluino mass is related to the neutralino mass via the universality condition, the

97.5%C.L. lower limit gives $m_{\tilde{g}} > 477$ GeV and the maximum can exceed 5 TeV. However we have $M_{\tilde{g}} < 3.3$ TeV with 84% C.L., which is slightly beyond the reach of the LHC with maximum luminosity.

- As mentionned before, squark masses are in the TeV range. Because of the universality assumption on squark masses the mixing in the stop sector implies that the stop is the lightest squark. We find $m_{\tilde{t}_1} > 1130$ GeV. Squark masses can reach all the way to the upper end of the range of the scan, 4TeV. There is no guarantee that squarks are within the reach of the LHC.

- Slepton masses reach almost all the way to 4TeV. Since masses of sleptons and gauginos are uncorrelated, a large fraction of scenarios have $m_{\tilde{l}_{1,2}} > m_{\chi_2^0}, m_{\tilde{\chi}_1^+}$ (around 75% of allowed scenarios). For these scenarios the preferred decay channel of $\tilde{\chi}_2^0$ is three body and has a branching fraction around 3% into each flavour of charged lepton. In this model all slepton masses are identical except for mixing effect so only one mass is displayed in Fig. 4

The higgsino fraction of the LSP strongly influences the properties of the DM, $f_H = |N_{13}|^2 + |N_{14}|^2$ where the neutralino mixing matrix is defined in the basis $\tilde{\chi}_1^0 = N_{11}\tilde{B} + N_{12}\tilde{W} + N_{13}\tilde{H}_1 + N_{14}\tilde{H}_2$. The higgsino fraction spans a wide range $3.4 \times 10^{-4} < f_H < 0.66$ at 95%C.L. The distribution is peaked around $0.15 < f_H < 0.35$. A small higgsino fraction is found either for light LSP's and for LSP's annihilating near a Higgs resonance. The higgsino fraction has an impact on the spectrum and in particular on the mass difference $m_{\tilde{\chi}_1^+} - m_{\tilde{\chi}_1^0}$. A large mass difference is expected for a small higgsino fraction (since in that case $m_{\tilde{\chi}_1^+}/m_{\tilde{\chi}_1^0} \approx 2$) whereas when $f_H > 0.15$, $m_{\tilde{\chi}_1^+} - m_{\tilde{\chi}_1^0} < M_W$ and $m_{\tilde{\chi}_2^0} - m_{\tilde{\chi}_1^0} < M_Z$. This means that for a large number of scenarios that satisfy this condition the decay channels $\tilde{\chi}_1^+ \to \tilde{\chi}_1^0 W$, $\tilde{\chi}_2^0 \to \tilde{\chi}_1^0 Z$ are forbidden and only 3-body decays are possible since sleptons are often heavier than the chargino.

Table 5: Range of predictions for observables

Observable	68% C.L.		95% C.L.	
Ωh^2	0.102	0.123	0.091	0.133
$\delta a_\mu \times 10^{10}$	1.49	27.2	-1.45	37.5
$B(B \to X\gamma) \times 10^4$	3.19	3.62	3.08	3.86
$B(B_s \to \mu^+\mu^-) \times 10^9$	1.82	3.31	1.48	20.4
$R(B \to \tau\nu)$	0.698	0.981	0.382	0.997
$\sigma_{\chi p}^{SI}$ (pb)	2.51×10^{-10}	6.76×10^{-8}	9.77×10^{-12}	2.24×10^{-7}

4.3 Other observables

Form the allowed parameter space we then examine the predictions for the observables used in the fit together with the direct detection cross-section.

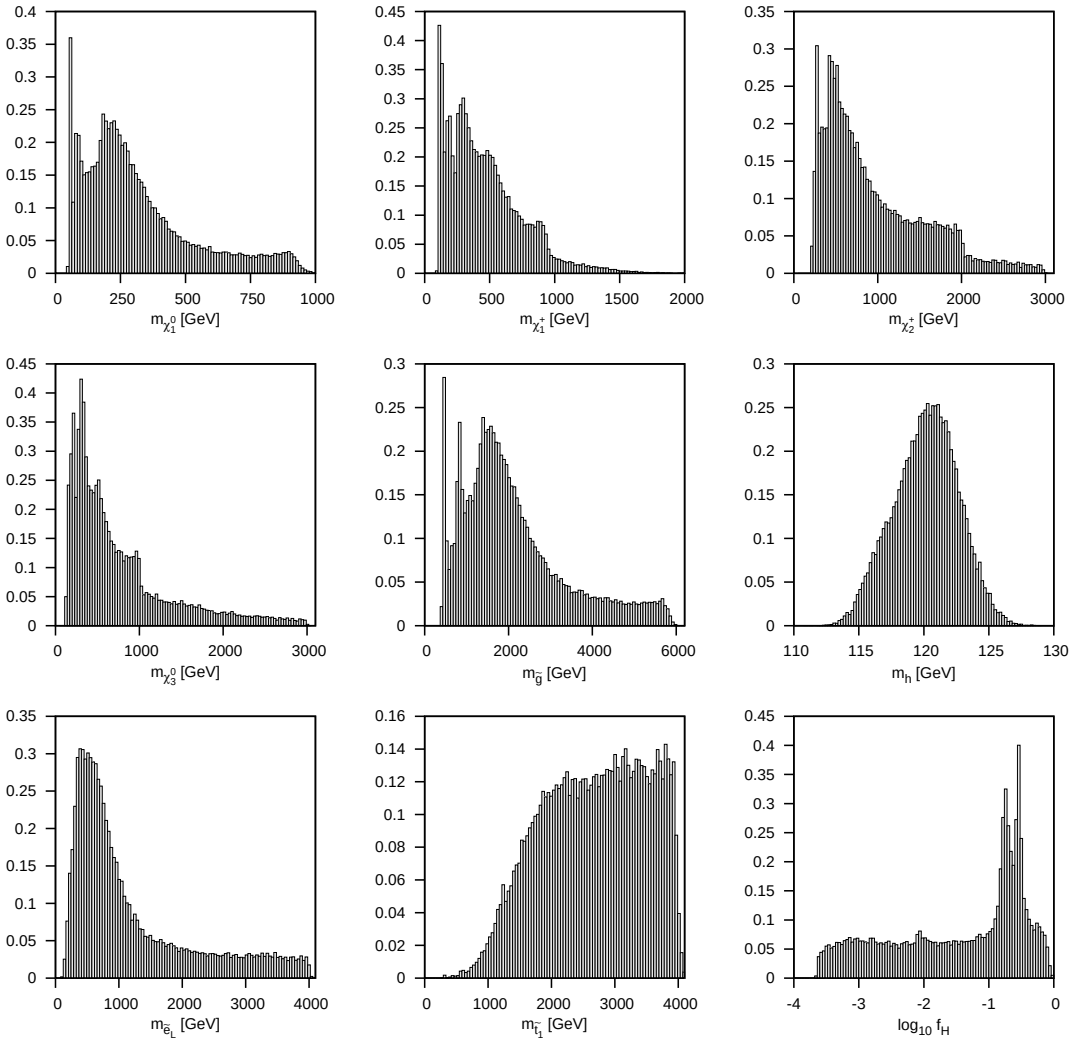

Figure 4: Distributions for sparticle masses: $m_{\tilde{\chi}_1^0}, m_{\tilde{\chi}_1^+}, m_{\tilde{\chi}_3^0}, m_{\tilde{\chi}_2^+}$, $m_{\tilde{g}}$, $m_h, m_{\tilde{e}_L}, m_{\tilde{t}_1}$ and for the higgsino fraction, f_H. There is a scale factor of 10^6 on the y-axis.

- The observables Ωh^2 and $B(b \to s\gamma)$ are well distributed around the central values used in the fit. As expected, $B(b \to s\gamma)$ lies near the upper end of the allowed range for small M_A, μ, M_2 and $M_{\tilde{l}}$ and are enhanced at very large values of $\tan\beta$.

- The branching ratio $B(B_s \to \mu^+\mu^-)$ is peaked around 2.5×10^{-9} although a long tail extends to $2. \times 10^{-8}$ at 95%C.L. Values near the upper limit are found for $M_A < 600$ GeV, $\tan\beta > 50$, for not too heavy charginos, $m_{\tilde{\chi}_1^+} < 750$ GeV and for a LSP with a small higgsino fraction, $f_H < 0.05$.

- At 97.5%C.L., $R(B \to \tau\nu) > 0.38$, as for other B-physics observables, the largest suppression to $R(B \to \tau\nu)$ are found for small M_A, μ, M_2 and $M_{\tilde{l}}$ as well as for $\tan\beta > 50$.

- The muon anomalous magnetic moment extends over more than an order of magnitude and in particular can include negative values. The peak of the distribution lies near 10^{-10}, much below the central experimental value we have used indicating that our model does not provide a good fit to this observable. Large deviations in

δa_μ are found for light sleptons and neutralinos/charginos, this is why a better fit to the data is found for low values of M_2 and $M_{\tilde{l}}$. This is illlustrated in Fig. 7a,b. This observable also plays a role in setting the upper limit on the neutralino/chargino masses.

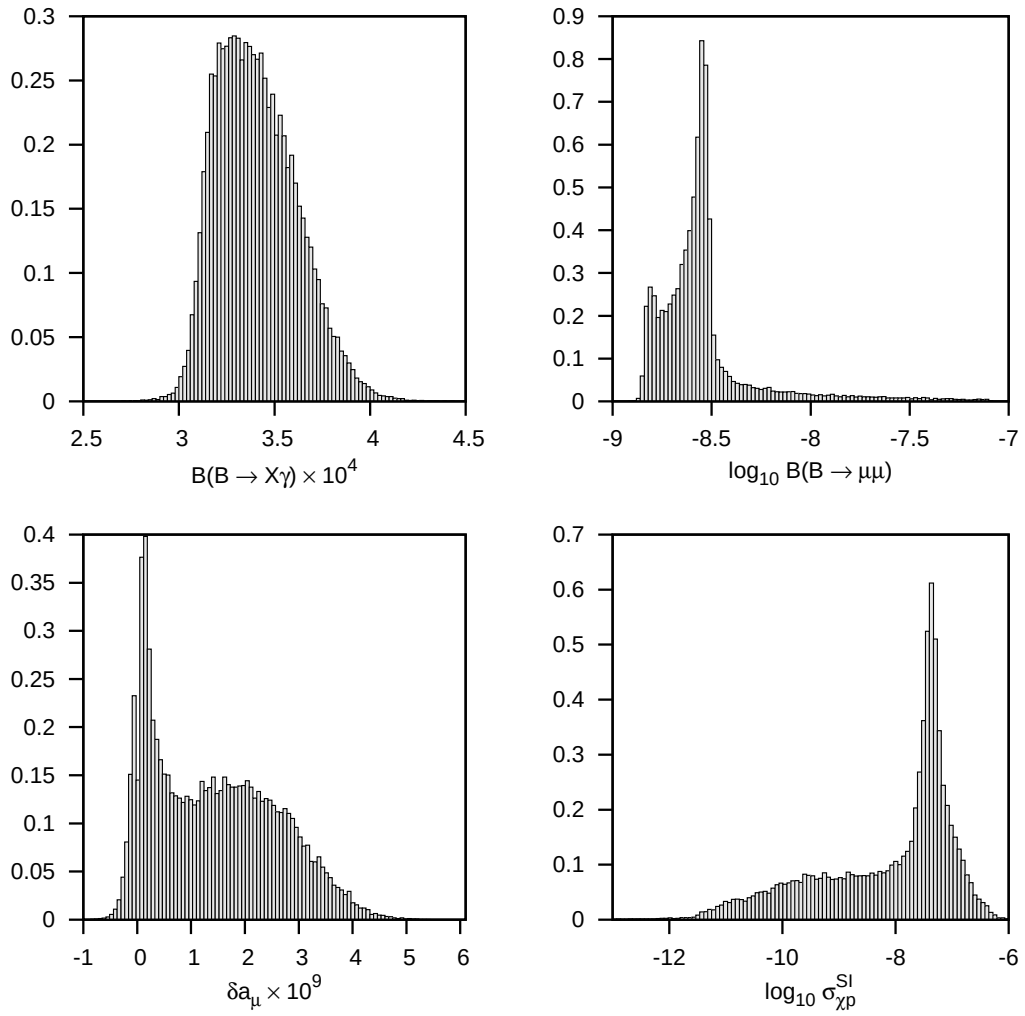

Figure 5: Distributions for $B(b \to s\gamma), B(B_s \to \mu^+\mu^-), \delta a_\mu, \sigma^{SI}_{\chi p}$. The y-axis is in units of 10^6.

Note that if δa_μ turns out to be consistent with the SM prediction, as indicated by some preliminary results [39], the distributions for $M_2, M_{\tilde{l}}$ would shift to larger values. The dependence of the B-observables on some of the most relevant parameters are displayed in Fig. 7c-i, in particular the enhancement with the light pseudoscalar mass for $B(B_s \to \mu^+\mu^-), B(b \to s\gamma), R(B \to \tau\nu)$. In fact a heavy pseudoscalar leaves little prospects for observing large deviations in B-observables, $M_A > 1$ TeV implies $B(B_s \to \mu^+\mu^-) < 5 \times 10^{-9}$ and $R(B \to \tau\nu) > 0.70$. Similarly small values of $\tan\beta$, for example $\tan\beta < 20$ implies $B(B_s \to \mu^+\mu^-) < 2.5 \times 10^{-9}$ and $R(B \to \tau\nu) > 0.85$. The potential enhancement at large values of $\tan\beta$ is illustrated only for $B(B_s \to \mu^+\mu^-)$. The largest values for $B(B_s \to \mu^+\mu^-)$ are also found at low values of M_2, they are therefore correlated with large deviations in δa_μ [40].

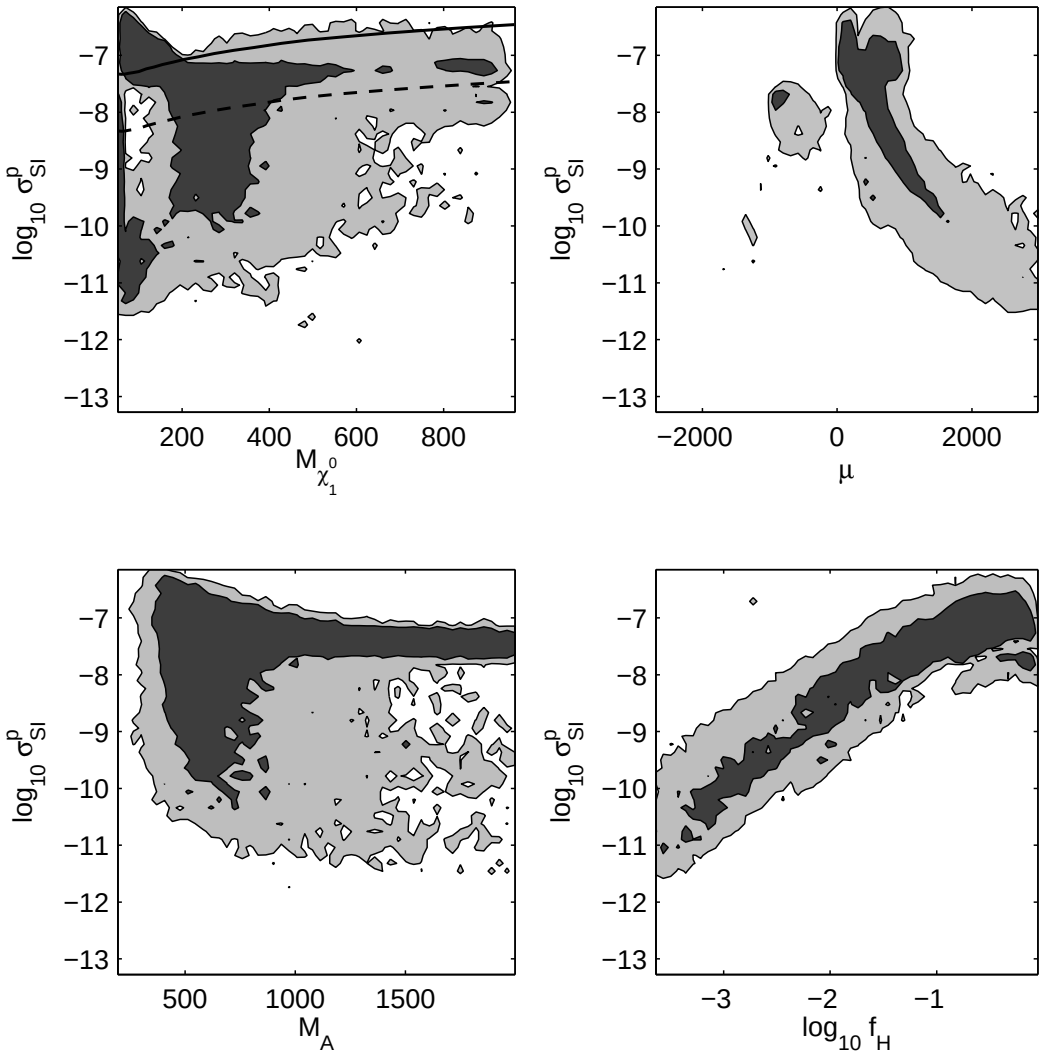

Figure 6: Predictions for elastic scattering cross sections as a function of $m_{\tilde{\chi}_1^0}$, μ, M_A and f_H. Default values of micrOMEGAs for the quark content of the nucleon are taken. On the top-left plot the CDMS-II exclusion is shown by a solid line, while the dashed line show the factor 10 improved limits.

The predictions for the neutralino nucleon elastic scattering, $\sigma_{\chi p}^{SI}$, vary over 5 orders of magnitude. The distribution peaks at values near the experimental upper limit, see Fig. 5 and can even exceed the present limit. The LSP mass dependent CDMS limit is displayed in Fig. 6a [2]. The light Higgs exchange in general dominate SI interactions. Therefore large cross sections are expected when the LSP has a large coupling to the light Higgs, this means some higgsino component, Fig. 6b,d. For example a LSP with a higgsino component $f_H > 0.2$ necessarily implies $\sigma_{\chi p}^{SI} > 3.2 \times 10^{-9}$ pb. These values will be probed in the near future with for example Xenon100 [12]. On the other hand a pure bino LSP has a cross section at least two orders of magnitude below the experimental limit. The second Higgs scalar as well as squarks can also contribute significantly when they have a mass comparable to the LSP. There is however no direct correlation between the direct detection rate and M_A. Note that the enhancement of the heavy Higgs contribution relative to the light Higgs expected at large values of $\tan\beta$ is tamed because the pseudoscalar is always

much heavier than the light Higgs (recall that $M_A > 370$ GeV).

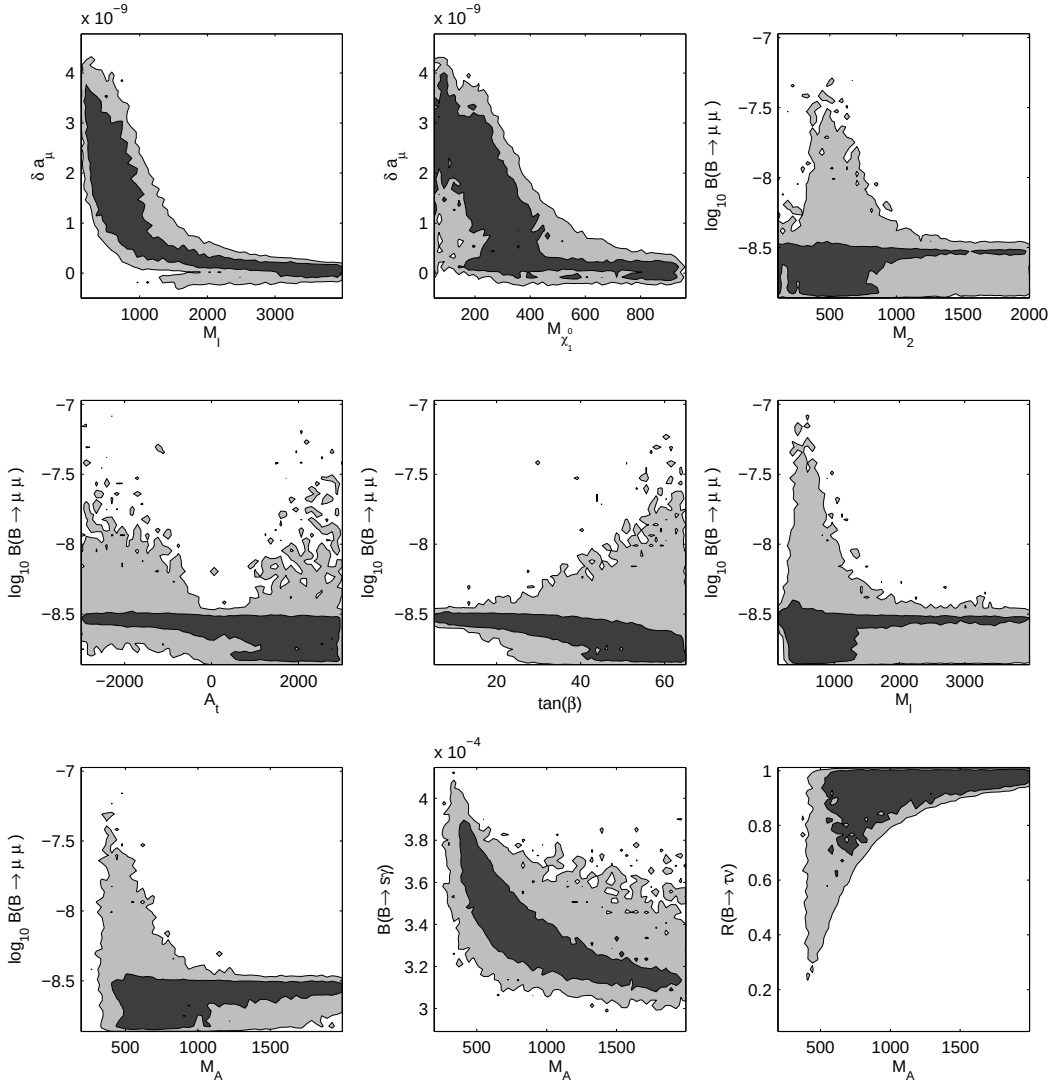

Figure 7: 2D contours for some observables, from top left to bottom right: a) $\delta a_\mu - M_{\tilde{l}}$ b) $\delta a_\mu - m_{\tilde{\chi}_1^0}$ c) $B(B_s \to \mu^+\mu^-) - M_{\tilde{l}}$ d) $B(B_s \to \mu^+\mu^-) - A_t$ e)$B(B_s \to \mu^+\mu^-) - \tan\beta$ f) $B(B_s \to \mu^+\mu^-) - M_A$ g)$B(B_s \to \mu^+\mu^-) - M_2$ h)$B(b \to s\gamma) - M_A$ i) $R(B \to \tau\nu) - M_A$. The 68%C.L. is in dark grey and 95%C.L. in light grey.

4.4 Complementarity of different LHC searches and direct dark matter searches

From the above discussion, it is clear that B-physics observables, δa_μ, direct detection as well as direct particle searches at LHC are sensitive to different sectors of the MSSM. Direct searches at LHC are especially powerful to probe the coloured sector while heavy Higgs searches probe the large $\tan\beta$. Direct detection probes best the higgsino LSP.

To illustrate quantitatively the complementarity of the various new physics signals at LHC and in direct detection we compute the fraction of models in the allowed parameter space that lead to a signal in 4 different channels: direct searches of sparticles at LHC, searches for heavy Higgs at LHC, deviation in $B(B_s \to \mu^+\mu^-)$ and DM direct detection. Here we choose $B(B_s \to \mu^+\mu^-)$ as a representative observable from the B-sector to simplify the discussion. The same exercice with another B-observables would lead to a similar conclusion. The signal in each channel is define as follows. We assume that coloured sparticles are within reach at LHC-14TeV if their mass is below 2 TeV. This corresponds roughly to the reach for gluinos when squarks are heavy and $\mathcal{L} = 60 fb^{-1}$ [16, 17]. This value for the squarks reach is conservative but we use it for simplicity, recall that with a high luminosity, $\mathcal{L} = 300 fb^{-1}$, coloured sparticles can be discovered up to 3 TeV. To define the discovery reach for the heavy Higgs we use the results of the CMS study which gives the discovery region in the $\tan\beta - M_A$ plane for $\mathcal{L} = 30 fb^{-1}$ [17]. This is based on the associated production of a Higgs with b-quarks, $gg, qq \to b\bar{b}h$ with the Higgs decaying into tau pairs. In the MSSM, this process is accessible only at large values of $\tan\beta$ because of the $\tan\beta$-enhanced couplings of the heavy Higgs to $b\bar{b}, \tau\bar{\tau}$ pairs. For example the pseudoscalar mass can be probed up to $M_A < 800$ GeV for $\tan\beta$=50.

For the process $B_s \to \mu^+\mu^-$ we assume the value for the branching $B(B_s \to \mu^+\mu^-) < 5\times10^{-9}$ which will be probed even with a low luminosity at the LHC. Finally for the elastic scattering cross section our definition of a signal corresponds to one order of magnitude improvement over the current CDMS limit [2]. With various experiments increasing their sensitivities regularly, this level should be reached in the near future [12].

Table 6: Prospects for Higgs searches, direct detection and $B(B_s \to \mu^+\mu^-)$ in scenarios with heavy coloured sparticles, $m_{\tilde{q}}, m_{\tilde{g}} > 2$ TeV

Heavy Higgs at LHC	$\sigma^{SI}_{\chi p}$(pb)	$B(B_s \to \mu^+\mu^-)$	
		$> 5.\times10^{-9}$	$< 5.\times10^{-9}$
Yes	20.6% ($> 10^{-9}$)	5.6%	15%
24.2%	3.6%($< 10^{-9}$)	1.7%	1.9%
No	54.9%($> 10^{-9}$)	0.3%	54.6%
75.8%	20.9%($< 10^{-9}$)	0.7%	20.2%

First we consider the case where sparticles are too heavy to be accessible at LHC, in these scenarios it is clearly essential to consider alternative signals of new physics and/or dark matter. In fact a large number of the allowed scenarios (almost 29%) predict a heavy coloured spectrum. We will refer to this as set A in the next section. This

is easily explained by the fact that no observable (except weakly for δa_μ) requires a supersymmetric contribution as long as the DM can give the proper relic abundance. The best alternative at LHC for a sign of physics beyond the standard model would be the search for a heavy Higgs [2] with nearly 24.2% of scenarios predicting a signal while few deviations from the SM in $B(B_s \to \mu^+\mu^-)$ are expected (only in 5.6% of the total number of scenarios in set A). Furthermore signals in B-physics are mostly found in scenarios for a light pseudoscalar Higgs and very large values of $\tan\beta$ where one also has a heavy Higgs signal. The complementarity between the direct detection and collider searches is clearly evident in Table 6. Nearly half (54.9%) the models lead to a signal only in direct detection experiments and about 20.6% of models predict a signal in both the Higgs and the direct detection. Conversely if no signal in direct detection is observed in the near future the model would be severely constrained (with 24.5% of scenarios remaining). Of course this statement should be modulated by the fact that there are large theoretical and astrophysical uncertainties in the prediction of the neutralino proton scattering cross section. Combining all the channels we are left with a small fraction of models with no signal in SUSY or Higgs searches at colliders, B physics or direct detection, the fraction corresponds to 20.2% of the subset with heavy sparticles which means about 6% of the sample of allowed scenarios. We have also checked that there are no other SUSY signals at LHC in these scenarios with heavy squarks and gluinos. We have computed the trilepton signal for direct neutralino/chargino production, $pp \to \tilde{\chi}_i^0 \tilde{\chi}_1^+ \to 3l + E_T^{miss}$ and found a maximum cross section of a few fb at $\sqrt{s} = 14$ TeV. The reasons for the small cross section are the heavy squarks and the heavy neutralinos and charginos, the (97.5%C.L.) lower limits are $m_{\tilde{\chi}_1^0}, m_{\tilde{\chi}_2^0}, m_{\tilde{\chi}_3^0} > 285, 366, 371 >$ GeV and $m_{\tilde{\chi}_1^+} > 354$ GeV. The direct production of sleptons is also below the LHC reach for $30 fb^{-1}$ since the lower limit on slepton masses are $m_{\tilde{e}_L}, m_{\tilde{e}_R} > 300$ GeV.

Table 7: Prospects for Higgs searches, direct detection and $B(B_s \to \mu^+\mu^-)$ in scenarios with light coloured sparticles, $m_{\tilde{q}} < 2$ TeV and $m_{\tilde{g}} < 2$ TeV

Heavy Higgs at LHC	$\sigma_{\chi p}^{SI}$(pb)	$B(B_s \to \mu^+\mu^-)$	
		$> 5. \times 10^{-9}$	$< 5. \times 10^{-9}$
Yes	21.9% ($> 10^{-9}$)	7.2%	14.7%
24.5%	2.7%($< 10^{-9}$)	1.6%	1.1%
No	53.7%($> 10^{-9}$)	0.6%	53.1%
75.5%	21.8%($< 10^{-9}$)	1.1%	20.7%

The results for the case where sparticles are accessible at LHC leads to roughly the same conclusion, see Table 7. One difference is a small increase in the fraction of models that predict an observable deviation in $B(B_s \to \mu^+\mu^-)$. This is particularly true if squarks below the 2TeV scale are present. In the case where a heavy Higgs and squarks are accessible at LHC, more than 35% of the models also predict $B(B_s \to \mu^+\mu^-) > 5. \times 10^{-9}$.

[2]Here we have not included the possibility of discovering SUSY particles in Higgs decays

4.5 Impact of improved sensitivity

Rather than just looking at the discovery potential we also examine the impact of a signal in the near future in direct detection or in $B(B_s \to \mu^+\mu^-)$. First let us comment on the impact of the present CDMS limit on direct detection. Recall that because of the astrophysical and nuclear uncertainties we have not used this observable in the fit. We applied this constraint a posteriori on the selected models and looked at the impact on the SUSY spectrum. The most noticeable effect of this constraint is that it removes some models with $65 < m_{\tilde{\chi}_1^0} < 170$ GeV especially when those models have a large value for the higgsino fraction f_H. Models with $m_{\tilde{\chi}_1^0} \approx 50$ GeV that have a small higgsino fraction are not affected. Furthermore some of the models with low values of M_A and large $\tan\beta$ are disfavoured. To have an indication of the impact of a signal in direct detection we then considered the case of a signal $\sigma_{\chi p}^{SI} = 1. \times 10^{-8}$ pb and allowed a factor 3 theoretical uncertainty. With such a measurement one could constrain the allowed parameter space although no specific correlation with other observables are observed, only a lower bound on the LSP higgsino fraction is found.

We have also considered the impact of a signal at the Tevatron in $B(B_s \to \mu^+\mu^-)$, say $B(B_s \to \mu^+\mu^-) > 1.8 \times 10^{-8}$ which represents the ultimate reach of Tevatron [41]. We found that in this case a lower bound on $\tan\beta > 32$ with 97.5%C.L could be extracted (though a tail extends till $\tan\beta \sim 18$) and furthermore that a heavy Higgs signal at LHC would almost be guaranteed (in 94.6% of the scenarios). Finally the models with a signal within the Tevatron reach in $B(B_s \to \mu^+\mu^-)$ all predict a small cross section in the trilepton channel ($\sigma_{lll}^{\rm TeV} < 0.1$ fb) even before applying cuts. This points towards a complementarity between the two channels as was found in the MSSM [42], although as we have mentionned before only a small fraction of the MSSM-UG models are within the Tevatron reach for the trileptons.

5 LHC forecasts

At last we examine in more details the SUSY signatures at the LHC. For this we split the scenarios allowed at 95% C.L. in different sets according to which sparticles are within the reach of the LHC. We have already mentionned that a significant fraction (28.7%) of our scenarios predict a coloured spectrum that is just too heavy (set A). Another large fraction (30.5%) corresponds to the case where the gluino is the only coloured sparticle that could be discovered at LHC (set B) while a squark is also within reach in 22.0% (set C). In 19% of our scenarios (set D) only squarks are accessible. The main difference from the CNMSSM is that in the latter the squark masses receive an important contribution from M_3 due to the renormalization group running so the cases where only a gluino is accessible at LHC are confined to the focus point region. The precise fraction of models that have sparticles within reach of the LHC do depend on the range on the parameters used in the scan. In particular it is clear that a wider range for the squark masses would have lead to a larger fraction of models with squarks too heavy to be produced at the LHC.

For two sets of scenarios we then examine the main branching fractions of sparticles concentrating on squarks, gluinos and on the neutralino/charginos produced in their decay. Our goal is to point out the different decay channels available. We do not attempt to analyse the feasibility of extracting signals over background in our scenarios, this is beyond

the scope of this paper.

Note that in some scenarios, the chargino/neutralino can be produced directly leading to a signal in the trilepton channel, $p\bar{p} \to \tilde{\chi}_i^0 \tilde{\chi}_1^+ \to 3l + E_T^{miss}$. We do not here analyse direct production specifically but we have checked that the Tevatron only weakly constrained our allowed scenario, only about 1 per-mil of our models have a trilepton cross section $\sigma(3l + E_T^{miss}) > 0.0.08$ pb before applying cuts.

5.1 Scenarios where $m_{\tilde{g}} < 2$TeV, $M_{\tilde{q}} > 2$ TeV.

In the MSSM-UG the scenarios where only gluinos are accessible at LHC represent a large fraction of the scenarios that provide a good fit to the data. To examine the characteristic decay chains in these scenarios, we have, for each point in our MCMC chain, computed the branching ratios of gluinos into neutralino/charginos as well as the 2- and 3-body branching ratios of $\tilde{\chi}_2^0$ and $\tilde{\chi}_3^0$ with `micrOMEGAs`. The decay chains involving a chargino can be dominant but we concentrate on the heavy neutralinos because the leptonic decay mode provide a clear signature and the kinematic endpoint in the lepton invariant mass distribution further allow for a determination of the mass difference of the heavy neutralino with the LSP.

In these scenarios the squarks are heavy so the gluino decays only via 3-body, $\tilde{g} \to \tilde{\chi}_i^+ f f'$ or $\tilde{g} \to \tilde{\chi}_i^0 f \bar{f}$ leading to final states with many jets as well as missing energy from the LSP. The branching fraction into third generation quarks is particularly relevant since it has been shown [43, 44] that requiring tagged b-quark jets in the final state helped reduce the SM background and thus could extend the LHC reach in this channel. In our sample scenarios, the total branching fraction for 3-body decays of gluinos into third generation quarks (t and b) $B(\tilde{g} \to \chi Q Q') = B_{gQQ}$ varies over a wide range, from $0.1 - 0.8$ and features two peaks around 25% and 70%, see Fig. 8a.[3] The $\tilde{\chi}_2^0, \tilde{\chi}_3^0$ channels each contribute below 20%, see Fig. 8b. The larger branching fractions B_{gQQ} are found for low values of μ, see Fig. 9, this is mainly because in this case all charginos and neutralinos can be produced in gluino decays and contribute significantly (especially charginos). The branching fraction B_{gQQ} also increases with $\tan\beta$, this is because of the enhanced coupling of the higgsino to $\tilde{b}b$.

Next we have computed the decay modes of the $\tilde{\chi}_2^0$ and $\tilde{\chi}_3^0$. The $\tilde{\chi}_2^0$ decays dominantly via 3-body, the branching fraction of neutralinos into each fermion pair is typical of the Z decay (around 3% for each leptonic mode), see Fig. 10. In some scenarios the two-body leptonic channels are accessible, in this case the $\tilde{\chi}_2^0$ either decay exclusively into the ligthest slepton (the stau) or into all sleptons including the invisible mode into sneutrinos, see Fig. 10b. Finally the decay channels into a gauge or Higgs boson and the LSP dominate for sufficient mass splitting between the neutralinos, the dominant mode is $\tilde{\chi}_2^0 \to \tilde{\chi}_1^0 h$ unless only the Z is kinematically accessible. For $\tilde{\chi}_3^0$ a larger fraction of scenarios have 2-body decay modes, in particular the decays into neutral and charged gauge bosons, $\tilde{\chi}_3^0 \to \tilde{\chi}_1^0 Z$, or $\tilde{\chi}_1^+ W$. Decays into sleptons are as before confined to the scenarios with light sleptons, Fig. 11.

Finally we have compiled the fraction of models (among set B only) that feature each dominant decay mode, the results are presented in Table 8. The largest sample (35%) corresponds to both neutralinos decaying into 3-body channels. In these scenarios

[3] For reference recall that in a typical focus point scenario the branching ratios of gluinos into third generation quarks reach 72% [45].

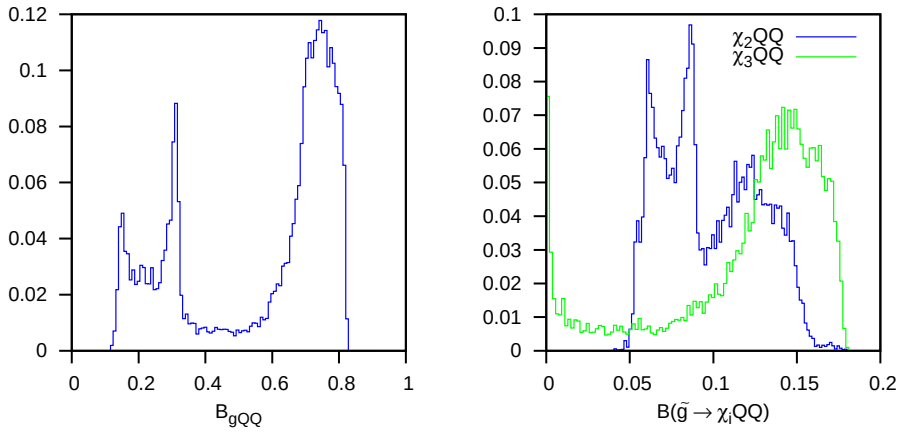

Figure 8: Distribution of the gluino branching fractions in third generation quarks a)B_{gQQ} b) $Br(\tilde{g} \to \tilde{\chi}_i^0 QQ)$. There is a scale factor of 10^6 on the y-axis.

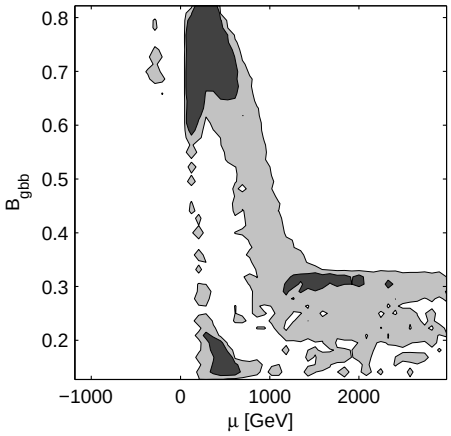

Figure 9: B_{gQQ} as a fuction of μ parameter.

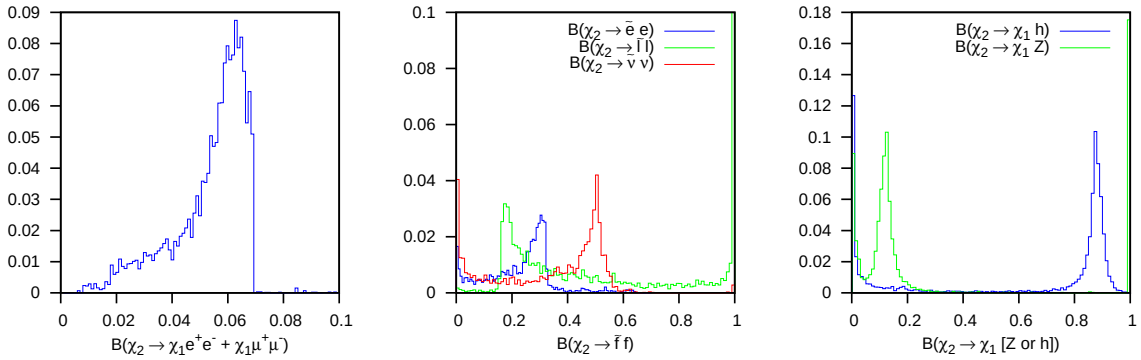

Figure 10: Distribution of $\tilde{\chi}_2^0$ branching fractions for the channels a) $\tilde{\chi}_1^0 e^+e^-(\mu^+\mu^-)$ b) $\tilde{l}l$ c) $\tilde{\chi}_1^0 Z, \tilde{\chi}_1^0 h$. There is a scale factor of 10^6 on the y-axis.

$\mu < 350$ GeV, $\mu - M_1$ is small and the LSP has a significant higgsino component so that the direct detection rate is large ($\sigma_{\chi p}^{SI} > 7 \times 10^{-9}$ pb). The scenarios where $\tilde{\chi}_3^0$ instead has 2-body decays also have in general a LSP with an important higgsino component and a large $\sigma_{\chi p}^{SI}$ except when $\tilde{\chi}_3^0 \to \tilde{\chi}_1^+ W^-$ is the dominant channel. Then we found

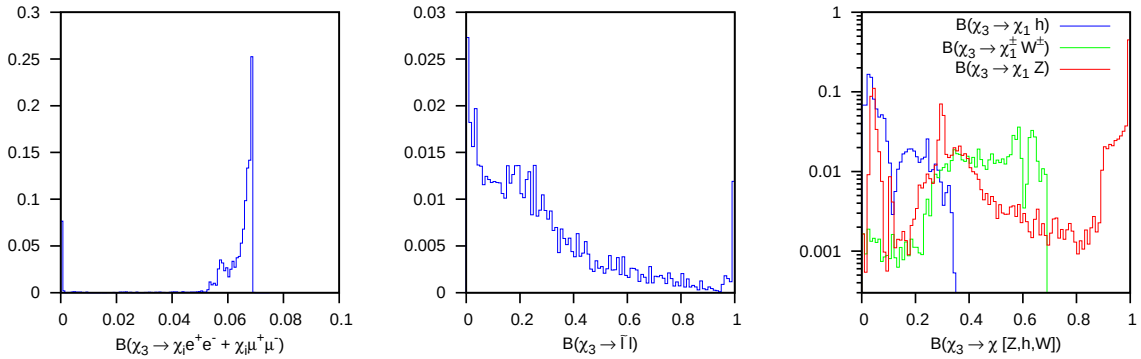

Figure 11: a) Distribution of $\tilde{\chi}_3^0$ branching fractions for the channels a) $\tilde{\chi}_i^0 e^+e^-, \mu^+\mu^-$ b) $\tilde{l}l$ c) $\tilde{\chi}_1^0 Z, \tilde{\chi}_1^0 h, \tilde{\chi}_1^+ W$. There is a scale factor of 10^6 on the y-axis.

Table 8: Dominant decay mode of $\tilde{\chi}_2^0$ and $\tilde{\chi}_3^0$ in models with $m_{\tilde{g}} < 2$ TeV and $M_{\tilde{q}} > 2$ TeV and fraction of allowed models corresponding to each dominant decay mode.

$\tilde{\chi}_2^0$	$\tilde{\chi}_3^0$	Fraction of models
$\tilde{\chi}_1^0 f\bar{f}$	$\tilde{\chi}_i^0 f\bar{f}$	35.2%
$\tilde{\chi}_1^0 f\bar{f}$	$\chi_1^{\pm}W^{\mp}$	4.2%
	$\chi_i Z, \chi_i h$	8.6%
	$\tilde{l}l$	0.2%
$\tilde{\chi}_1^0 Z$	$\chi_1^{\pm}W^{\mp}$	6.0%
$\tilde{\chi}_1^0 h$	$\chi_i Z$ (or $\chi_1^{\pm}W^{\mp}$)	14.4%
$\tilde{l}l$	$\tilde{l}l$	4.6%
	$\chi_1^{\pm}W^{\mp}$	6.1%
$\tilde{\chi}_1^0 f\bar{f}$	-	3.8%
$\tilde{\chi}_1^0 Z$	-	2.8%
$\tilde{\chi}_1^0 h$	-	6.7%
$\tilde{l}l$	-	5.0%

predominantly $m_{\tilde{\chi}_1^0} \approx 60$ GeV with a bino LSP annihilating efficiently through a light Higgs resonance.

A large number of scenarios (31% of set B) correspond to both $\tilde{\chi}_2^0$ and $\tilde{\chi}_3^0$ having 2-body decay modes. The case where the dominant decay mode is $\tilde{\chi}_2^0 \to \tilde{\chi}_1^0 Z$ correspond to a small value for $\mu - M_1$, this means a dominantly higgsino LSP. In general though the dominant modes are $\tilde{\chi}_2^0 \to \tilde{\chi}_1^0 h$ and $\tilde{\chi}_3^0 \to \tilde{\chi}_1^0 Z$ unless sleptons are light. In nearly 19% of sceanrios B, μ is large and the $\tilde{\chi}_3^0$ which is higgsino cannot be produced in gluino decays. The $\tilde{\chi}_2^0$ decays predominantly via 2-body channels, $\tilde{l}l, \chi_1 h$ or $\chi_1 Z$ or into 3-body $\tilde{\chi}_2^0 \to \tilde{\chi}_1^0 f\bar{f}$ with the leptonic mode offering a robust signature. Typically in these

scenarios the elastic scattering cross sections is small apart from the cases where the heavy Higgs is light enough to contribute significantly.

In conclusion, although the focus point like scenario with gluinos decay with large fraction into b quarks and leptonic 3 body decays of $\tilde{\chi}_2^0, \tilde{\chi}_3^0$ constitute the largest sample, the channels with two body decays of neutralinos are also very important. Among these cases where leptonic decays of $\tilde{\chi}_2^0$ dominate constitute 16% of our sample while those where the only final states include $Z(W)$ or h constitute about 30% of our sample. Note that the gluino only scenario could be quite challenging for the LHC especially if the gluino is near 2TeV. We have checked that the scenarios that would be accessible with a lower luminosity, say $m_{\tilde{g}} < 900$ GeV for $\mathcal{L} = 30\text{fb}^{-1}$, share the main features we have just described. Obviously because of the lighter spectrum a smaller fraction of scenarios have $\tilde{\chi}_3^0$ accessible in gluinos decays. Furthermore the fraction of scenarios with 2-body decays is smaller with for example hardly any scenario where both $\tilde{\chi}_2^0$ and $\tilde{\chi}_3^0$ decay via 2-body.

5.2 Scenarios where $M_{\tilde{q}} < 2$ TeV, $m_{\tilde{g}} > 2$ TeV

In the MSSM-UG a small fraction of allowed scenarios (set D) predicts that only squarks are lighter than 2TeV. In this case, the main contribution to SUSY production is direct production of squark pairs. In the MSSM-UG, the masses of sleptons and squarks are not correlated ,so sleptons are not always light enough to be produced in neutralino decays. The conventional SUSY searches which involve a decay chain with a neutralino $\tilde{q} \to \tilde{\chi}_2^0 j \to \tilde{l} l j \to \tilde{\chi}_1^0 \tilde{l} l j$ will be superseded by the two-body decays, $\tilde{\chi}_2^0 \to \tilde{\chi}_1^0 Z, \tilde{\chi}_1^0 h$ or $\tilde{\chi}_1^+ W$ or if kinematically forbidden by 3-body decays.

We have computed the branching fractions for squarks, taking as an example the $\tilde{u}_L$ and $\tilde{u}_R$. We have then looked for the dominant mode into either a chargino, a heavy neutralino or the direct decay into the LSP. In each case we have also examined the decay mode of the neutralinos and charginos that occur in the squark decays. The higgsino fraction of the LSP is an important factor that determines the dominant decay mode. We therefore analyse the dominant decay modes separately for the case of a bino, mixed or higgsino LSP. Note that a mixed LSP constitutes more than half of our sample of scenarios.

The right-handed squark decays mainly into the bino component which means that the dominant decay is in general $\tilde{u}_R \to u\tilde{\chi}_1^0$, leading to only jets and missing energy. The decay $\tilde{u}_R \to u\tilde{\chi}_3^0$ can occur only when the LSP is a higgsino ($f_H \gtrsim 50\%$) so that the $\tilde{\chi}_1^0$ channel is suppressed. In this case however the heavier neutralino decay mostly via 3 body decays into the lightest chargino or neutralino + jets leading again to signatures with jets and missing energy.

The left-handed quark which couples strongly to the wino and/or higgsino component has a wide variety of decay modes. The frequency of each dominant decay chain are displayed in Table 9 for each LSP configuration. For the bino LSP the dominant mode is usually $\tilde{u}_L \to d\tilde{\chi}_1^+$ with typical branching fractions around 60%. The chargino will decay either into $\tilde{\chi}_1^0 W$ or $\tilde{l} l'$ when light sleptons are present. The subdominant mode in those scenario is $\tilde{u}_L \to u\tilde{\chi}_2^0$ with $\tilde{\chi}_2^0 \to \tilde{l} l, \tilde{\chi}_1^0 Z, \tilde{\chi}_1^0 h$. The decay chains are similar to those of the CMSSM. In some cases the second chargino, a mixed higgsino/wino, is kinematically accessible and the dominant mode will be $\tilde{u}_L \to d\tilde{\chi}_2^+$ with subdominant decays into $\tilde{\chi}_4^0 u$ and $\tilde{\chi}_1^+ d$. $\tilde{\chi}_2^+$ will decay preferentially into $\tilde{\chi}_2^0 W$ or in other neutralinos as well as into $\tilde{l} l$. The Higgs can be produced in either $\tilde{\chi}_2^+ \to \tilde{\chi}_1^+ h$ or further in $\tilde{\chi}_2^0 \to \tilde{\chi}_1^0 h$. A fraction of

Table 9: Dominant decay chains for $\tilde{u}_L$ for a bino, mixed or higgsino LSP.

		bino	mixed	higgsino
		$f_H \leq 0.01$	$0.01 < f_H \leq 0.5$	$f_H > 0.5$
$\tilde{u}_L \to \tilde{\chi}_1^0\, u$		7.7%	2.5%	–
$\tilde{u}_L \to \tilde{\chi}_3^0\, u$	$\tilde{\chi}_3^0 \to \tilde{l}l$	-	-	0.3%
	$\tilde{\chi}_3^0 \to \tilde{\chi}_1^+ W$	-	-	0.3%
	$\tilde{\chi}_3^0 \to \tilde{\chi}_1^+ f'\bar{f}$	-	2.0%	7.4%
$\tilde{u}_L \to \tilde{\chi}_1^+ d$	$\tilde{\chi}_1^+ \to \tilde{\chi}_1^0 W$	12.4%	-	-
	$\tilde{\chi}_1^+ \to \tilde{l}l'$	8.9%	-	-
$\tilde{u}_L \to \tilde{\chi}_2^+ d$	$\tilde{\chi}_2^+ \to \tilde{\chi}_i^0 W$	2.7%	37.2%	2.5%
	$\tilde{\chi}_2^+ \to \tilde{\chi}_1^+ h$	-	1.0%	0.6%
	$\tilde{\chi}_2^+ \to \tilde{l}l'$	1.1%	12.5%	0.6%
Fraction of sample		32.8%	55.3%	11.9%

models (7.7%) feature the dominant decay into the LSP $\tilde{u}_L \to u\tilde{\chi}_1^0$. Because the squark $\tilde{q}_L$ has a suppressed rate to the bino, this channel is dominant only when other two-body channels are kinematically forbidden.

For a mixed LSP ($0.01 < f_H \leq 0.5$) the relative importance of the various decay channels shifts. The decay $\tilde{u}_L \to u\tilde{\chi}_1^0$ is dominant in less than 3% of the cases although because of the higgsino component of the LSP this can occur even when heavier neutralinos are kinematically accesssible. By far the most frequent dominant decay is $\tilde{u}_L \to d\tilde{\chi}_2^+$ with significant branching fractions in $u\tilde{\chi}_3^0$ or $d\tilde{\chi}_1^+$. The heavier chargino always has two-body decay modes, $\tilde{\chi}_2^+ \to \tilde{\chi}_i^0 W$ (preferably $\tilde{\chi}_2^0 W$) or $\tilde{\chi}_2^+ \to \tilde{\chi}_1^+ h$. The $\tilde{\chi}_2^0, \tilde{\chi}_3^0$ and $\tilde{\chi}_1^+$ in turn feature mostly 3-body decays. Note that decay modes into Higgs bosons $\tilde{\chi}_2^+ \to \tilde{\chi}_1^+ h$ can involve even the heavy Higgs bosons. As usual when light sleptons are present the decay $\tilde{\chi}_2^+ \to \tilde{l}l'$ can be dominant.

For the higgsino LSP ($f_H > 0.5$), the dominant mode is either $\tilde{\chi}_3^0 u$ or $\tilde{\chi}_2^+ d$ with some contributions from $\tilde{\chi}_2^+ d$ and $\tilde{\chi}_4^0 u$. The $\tilde{\chi}_2^+$ channel has similar decay chains as the mixed LSP except that the dominant mode is usually $\tilde{\chi}_2^+ \to \tilde{\chi}_2^0 W$ rather than channels involving Higgses. The $\tilde{\chi}_3^0$ can in a few cases decay via two-body, $\tilde{\chi}_1^+ W$ or $\tilde{l}l$, but in most cases it decays via three-body dominantly into $\tilde{\chi}_3^0 \to \tilde{\chi}_1^+ f f'$. These decays mainly give signatures into jets and missing energy. The $\tilde{\chi}_1^+$ produced in squark or neutralino decays will also decay via three body final states.

In summary $\tilde{q}_L$ decays dominantly into heavy charginos with further decay chains involving other chargino/neutralino states. Decay chains involving slepton production dominater only in 25% of scenarios. Finally recall that the elastic scattering cross section also differs significantly depending on the nature of the LSP giving an opportunity to correlate SUSY signals at LHC with those of direct detection. For the bino LSP, $\sigma_{\chi p}^{SI} < 10^{-9}$ pb while $\sigma_{\chi p}^{SI} > 10^{-9}(5 \times 10^{-8})$ pb for the mixed (higgsino) LSP.

We do not discuss in detail the case where both squarks and gluinos are below 2TeV. The decay chains can be rather complicated with the possibility of producing the gluino in squark decay and vice-versa. The case where the gluino is heavier than the squarks features the same decay chains for the squarks as the case just discussed.

6 Conclusion

Increasing the number of free parameters as compared to the CMSSM model has opened up the possibilities for supersymmetric scenarios that are compatible with all experimental constraints and this even maintaining the universality of gaugino mass. Although the parameter space of the model is still not very well constrained, we found that the most favoured models have a LSP of a few hundred GeV with a significant higgsino fraction ($> 10\%$). Contrary to the CMSSM case the higgsino LSP is not fully correlated with a very heavy squark sector although all our scenarios favour squarks above the TeV scale. A very light pseudoscalar is also disfavoured with $M_A > 370$ GeV, this means that large deviations from the SM in B-physics observables are expected only in a small fraction of allowed scenarios. Our favoured scenarios predict few signals at the Tevatron, the pseudoscalar Higgs as well as the coloured sector are too heavy to be accessed by direct searches. Only very few scenarios have a potentially large enough rate for trilepton searches at the Tevatron. The complementarity between future experiments to probe this class of models was emphasized. Even though SUSY or heavy Higgs signals are not guaranteed at LHC, the majority of allowed models predict at least one signal either at the LHC (including the flavour sector) or in future direct detection experiment. Furthermore the light Higgs is expected to be around 120GeV with SM-like couplings.

We have also explored the various dominant decay chains for gluinos and squarks that could be produced at LHC in the MSSM-UG as well as for the heavy neutralinos appearing in the decays of these coloured sparticles. We found that for models with gluinos accessible at LHC, a significant fraction of the heavy neutralinos produced decayed dominantly into a gauge or Higgs boson. Furthermore states which decayed into sleptons are rarely dominant. We also showed how the preferred squarks decay channels are determined to a large extent by the neutralino composition. Whether one can exploit these decay chains to determine some properties of the sparticles remains to be seen. In our analysis the relic density measurement plays the dominant role in constraining the model, since the relic density computation implicitly assumes a standard cosmological scenario, relaxing this requirement affects significantly the allowed parameter space of the model.

Finally we comment on the difference between our results and other recent analyses done within the framework of the MSSM with 24 parameters, either using a MCMC likelihood approach or applying 2σ constraints on each of the observables [26, 46]. First these studies were done in a more general model than the one we have considered, with in particular no universality condition on the gaugino masses. This means that the LSP can have a significant wino component and therefore is more likely to be at the TeV scale as was found in [27] using linear priors. Recall that a TeV scale wino annihilates efficiently into gauge bosons pairs. The analysis of [27] also emphasizes the prior dependence with a generally much lighter spectrum using log priors. This is due mostly to the poorly constrained parameter space [47, 48]. As in our analysis squarks and sleptons ran over the full range allowed in the scan and the pseudoscalar mass can be very heavy.

The analysis of [26] used a different statistical treatment but most importantly did not require that the neutalino explained all the DM in the universe (only an upper bound on Ωh^2 was imposed). This means that a large number of models with small mass splitting between the LSP and the NLSP appeared in the scan calling for a careful study of collider limits. In our approach such models are ruled out since they have $\Omega h^2 \ll 0.1$. This analysis further emphasized the light SUSY spectrum in their scans so naturally found preferred LSP mass below the TeV scale.

7 Acknowledgements

We thank J. Hamann for many useful discussions on the MCMC method. We acknowledge support from the Indo French Center fro Promotion of Advanced Scientific Research under project number 30004-2. This work was also supported in part by the GDRI-ACPP of CNRS and by the French ANR project `ToolsDMColl`, BLAN07-2-194882. The work of A.P. was supported by the Russian foundation for Basic Research, grant RFBR-08-02-00856-a and RFBR-08-02-92499-a.

References

[1] **XENON** Collaboration, J. Angle *et al.*, "First Results from the XENON10 Dark Matter Experiment at the Gran Sasso National Laboratory," *Phys. Rev. Lett.* **100** (2008) 021303, `arXiv:0706.0039 [astro-ph]`.

[2] **CDMS** Collaboration, Z. Ahmed *et al.*, "A Search for WIMPs with the First Five-Tower Data from CDMS," `arXiv:0802.3530 [astro-ph]`.

[3] **PAMELA** Collaboration, O. Adriani *et al.*, "An anomalous positron abundance in cosmic rays with energies 1.5.100 GeV," *Nature* **458** (2009) 607–609, `arXiv:0810.4995 [astro-ph]`.

[4] **The Fermi LAT** Collaboration, A. A. Abdo *et al.*, "Measurement of the Cosmic Ray e+ plus e- spectrum from 20 GeV to 1 TeV with the Fermi Large Area Telescope," `arXiv:0905.0025 [astro-ph.HE]`.

[5] **H.E.S.S.** Collaboration, F. Aharonian *et al.*, "The energy spectrum of cosmic-ray electrons at TeV energies," *Phys. Rev. Lett.* **101** (2008) 261104, `arXiv:0811.3894 [astro-ph]`.

[6] O. Adriani *et al.*, "A new measurement of the antiproton-to-proton flux ratio up to 100 GeV in the cosmic radiation," *Phys. Rev. Lett.* **102** (2009) 051101, `arXiv:0810.4994 [astro-ph]`.

[7] **WMAP** Collaboration, J. Dunkley *et al.*, "Five-Year Wilkinson Microwave Anisotropy Probe (WMAP) Observations: Likelihoods and Parameters from the WMAP data," *Astrophys. J. Suppl.* **180** (2009) 306–329, `arXiv:0803.0586 [astro-ph]`.

[8] **WMAP** Collaboration, D. N. Spergel *et al.*, "Wilkinson Microwave Anisotropy Probe (WMAP) three year results: Implications for cosmology," *Astrophys. J. Suppl.* **170** (2007) 377, arXiv:astro-ph/0603449.

[9] **SDSS** Collaboration, M. Tegmark *et al.*, "Cosmological Constraints from the SDSS Luminous Red Galaxies," *Phys. Rev.* **D74** (2006) 123507, arXiv:astro-ph/0608632.

[10] **CDF** Collaboration, T. Aaltonen *et al.*, "Search for new physics in the $\mu\mu + e/\mu + \not\!\!E_T$ channel with a low-p_T lepton threshold at the Collider Detector at Fermilab," *Phys. Rev.* **D79** (2009) 052004, arXiv:0810.3522 [hep-ex].

[11] **D0** Collaboration, V. M. Abazov *et al.*, "Search for associated production of charginos and neutralinos in the trilepton final state using 2.3 fb-1 of data," arXiv:0901.0646 [hep-ex].

[12] E. Aprile, L. Baudis, and f. t. X. Collaboration, "Status and Sensitivity Projections for the XENON100 Dark Matter Experiment," arXiv:0902.4253 [astro-ph.IM].

[13] **CDMS** Collaboration, T. Bruch, "Status and future of the CDMS experiment: CDMS-II to SuperCDMS," *AIP Conf. Proc.* **957** (2007) 193–196.

[14] **GLAST LAT** Collaboration, A. A. Moiseev, "Gamma-ray Large Area Space Telescope: Mission overview," *Nucl. Instrum. Meth.* **A588** (2008) 41–47.

[15] E. Mocchiutti *et al.*, "The PAMELA Space Experiment," arXiv:0905.2551 [astro-ph.HE].

[16] "ATLAS detector and physics performance. Technical design report. Vol. 2,". CERN-LHCC-99-15.

[17] **CMS** Collaboration, G. L. Bayatian *et al.*, "CMS technical design report, volume II: Physics performance," *J. Phys.* **G34** (2007) 995–1579.

[18] M. Artuso *et al.*, "B, D and K decays," *Eur. Phys. J.* **C57** (2008) 309–492, arXiv:0801.1833 [hep-ph].

[19] J. R. Ellis, S. Heinemeyer, K. A. Olive, A. M. Weber, and G. Weiglein, "The Supersymmetric Parameter Space in Light of B^- physics Observables and Electroweak Precision Data," *JHEP* **08** (2007) 083, arXiv:0706.0652 [hep-ph].

[20] H. Baer and C. Balazs, "Chi**2 analysis of the minimal supergravity model including WMAP, g(mu)-2 and b –¿ s gamma constraints," *JCAP* **0305** (2003) 006, arXiv:hep-ph/0303114.

[21] G. Belanger, F. Boudjema, A. Cottrant, A. Pukhov, and A. Semenov, "WMAP constraints on SUGRA models with non-universal gaugino masses and prospects for direct detection," *Nucl. Phys.* **B706** (2005) 411–454, arXiv:hep-ph/0407218.

[22] E. A. Baltz and P. Gondolo, "Markov chain Monte Carlo exploration of minimal supergravity with implications for dark matter," *JHEP* **10** (2004) 052, arXiv:hep-ph/0407039.

[23] B. C. Allanach and C. G. Lester, "Multi-Dimensional mSUGRA Likelihood Maps," *Phys. Rev.* **D73** (2006) 015013, arXiv:hep-ph/0507283.

[24] B. C. Allanach, C. G. Lester, and A. M. Weber, "The Dark Side of mSUGRA," *JHEP* **12** (2006) 065, arXiv:hep-ph/0609295.

[25] R. R. de Austri, R. Trotta, and L. Roszkowski, "A Markov chain Monte Carlo analysis of the CMSSM," *JHEP* **05** (2006) 002, arXiv:hep-ph/0602028.

[26] C. F. Berger, J. S. Gainer, J. L. Hewett, and T. G. Rizzo, "Supersymmetry Without Prejudice," *JHEP* **02** (2009) 023, arXiv:0812.0980 [hep-ph].

[27] S. S. AbdusSalam, B. C. Allanach, F. Quevedo, F. Feroz, and M. Hobson, "Fitting the Phenomenological MSSM," arXiv:0904.2548 [hep-ph].

[28] H. Baer, A. Mustafayev, S. Profumo, A. Belyaev, and X. Tata, "Direct, indirect and collider detection of neutralino dark matter in SUSY models with non-universal Higgs masses," *JHEP* **07** (2005) 065, arXiv:hep-ph/0504001.

[29] A. Bottino, F. Donato, N. Fornengo, and S. Scopel, "Size of the neutralino nucleon cross-section in the light of a new determination of the pion nucleon sigma term," *Astropart. Phys.* **18** (2002) 205–211, arXiv:hep-ph/0111229.

[30] G. Belanger, F. Boudjema, A. Pukhov, and A. Semenov, "Dark matter direct detection rate in a generic model with micrOMEGAs2.2," *Comput. Phys. Commun.* **180** (2009) 747–767, arXiv:0803.2360 [hep-ph].

[31] G. Bélanger *et al.* in preparation.

[32] Z. Zhang, "Muon g-2: a mini review," arXiv:0801.4905 [hep-ph].

[33] D. Mackay, *Information theory, Inference, and learning Algorithms*, Cambridge University Press,2003.

[34] B. C. Allanach, "SOFTSUSY: A C++ program for calculating supersymmetric spectra," *Comput. Phys. Commun.* **143** (2002) 305–331, arXiv:hep-ph/0104145.

[35] G. Belanger, F. Boudjema, A. Pukhov, and A. Semenov, "micrOMEGAs: Version 1.3," *Comput. Phys. Commun.* **174** (2006) 577–604, arXiv:hep-ph/0405253.

[36] G. Belanger, F. Boudjema, A. Pukhov, and A. Semenov, "micrOMEGAs2.0: A program to calculate the relic density of dark matter in a generic model," *Comput. Phys. Commun.* **176** (2007) 367–382, arXiv:hep-ph/0607059.

[37] M. Misiak *et al.*, "The first estimate of B(anti-B –¿ X/s gamma) at O(alpha(s)**2)," *Phys. Rev. Lett.* **98** (2007) 022002, arXiv:hep-ph/0609232.

[38] **D0** Collaboration, V. M. Abazov *et al.*, "Search for squarks and gluinos in events with jets and missing transverse energy using 2.1 fb^{-1} of $p\bar{p}$ collision data at $\sqrt{s} =$ 1.96- TeV," *Phys. Lett.* **B660** (2008) 449–457, arXiv:0712.3805 [hep-ex].

[39] M. Davier, "g-2," Talk presented at Tau'08, Novosibirsk,Russia.

[40] A. Dedes, H. K. Dreiner, and U. Nierste, "Correlation of B/s –¿ mu+ mu- and (g-2)(mu) in minimal supergravity," *Phys. Rev. Lett.* **87** (2001) 251804, arXiv:hep-ph/0108037.

[41] J. Lewis, talk presented at Moriond electrowek 2009, LaThuile, Italy, March 2009.

[42] A. Dedes, H. K. Dreiner, U. Nierste, and P. Richardson, "Trilepton events and $B/s \to \mu^+\mu^-$: No-lose for mSUGRA at the Tevatron?," arXiv:hep-ph/0207026.

[43] P. G. Mercadante, J. K. Mizukoshi, and X. Tata, "Using b-tagging to enhance the SUSY reach of the CERN Large Hadron Collider," *Phys. Rev.* **D72** (2005) 035009, arXiv:hep-ph/0506142.

[44] R. H. K. Kadala, P. G. Mercadante, J. K. Mizukoshi, and X. Tata, "Heavy-flavour tagging and the supersymmetry reach of the CERN Large Hadron Collider," *Eur. Phys. J.* **C56** (2008) 511–528, arXiv:0803.0001 [hep-ph].

[45] U. De Sanctis, T. Lari, S. Montesano, and C. Troncon, "Perspectives for the detection and measurement of Supersymmetry in the focus point region of mSUGRA models with the ATLAS detector at LHC," *Eur. Phys. J.* **C52** (2007) 743–758, arXiv:0704.2515 [hep-ex].

[46] S. Profumo and C. E. Yaguna, "A statistical analysis of supersymmetric dark matter in the MSSM after WMAP," *Phys. Rev.* **D70** (2004) 095004, arXiv:hep-ph/0407036.

[47] B. C. Allanach, K. Cranmer, C. G. Lester, and A. M. Weber, "Natural Priors, CMSSM Fits and LHC Weather Forecasts," *JHEP* **08** (2007) 023, arXiv:0705.0487 [hep-ph].

[48] R. Trotta, F. Feroz, M. P. Hobson, L. Roszkowski, and R. Ruiz de Austri, "The Impact of priors and observables on parameter inferences in the Constrained MSSM," *JHEP* **12** (2008) 024, arXiv:0809.3792 [hep-ph].